TRENDS IN SCIENCES 2025; 22(6): 9605 RESEARCH ARTICLE
https://doi.org/10.48048/tis.2025.9605

Synthesis and Evaluation of HKHK-PKKKRKV and Its Lipopeptide as New Gene Delivery Candidates

Nurul Muthia[1], Ace Tatang Hidayat[1,2], Tarwadi[3], Rani Maharani[1,2,*]

[1]Department of Chemistry, Faculty of Mathematics and Natural Sciences, Universitas Padjadjaran, Sumedang 45363, Indonesia
[2]Central Laboratory, Universitas Padjadjaran, Sumedang 45363, Indonesia
[3]Research Center for Vaccine and Drug Development, Badan Riset dan Inovasi Nasional (BRIN), South Tangerang 15314, Indonesia

([*]Corresponding author's e-mail: r.maharani@unpad.ac.id)

Received: 25 December 2024, Revised: 25 January 2025, Accepted: 5 February 2025, Published: 1 May 2025

Abstract

A major challenge in the delivery of genetic material is finding safe and effective vectors to deliver genetic material into target cells. Although virus-based vectors have proven to be effective in delivering genes to the cell nucleus, they often turn out to be harmful and interact with host cells. On the other hand, naturally available or chemically synthesized nonviral vectors are relatively safer but have low delivery efficiency. Research regarding the use of lipopeptide-based compounds as non-viral vectors for the delivery of genetic material is still limited. This study aims to synthesize NLS-based peptide, HKHK-PKKKRKV (P) and its lipopeptide, C16-HKHK-PKKKRKV (LP), and to evaluate their capability to transport genetic material into the nucleus *in vitro*. Synthesis of peptide and its lipopeptide was performed using the solid-phase method on 2-chlorotrityl chloride resin with Fmoc chemistry. HATU/HOAt was used as coupling reagents for amide bond formation between 2 amino acids, and DIC/Oxyma was used for fatty acid conjugation to the peptidyl resin. The yields of peptide and lipopeptide obtained were 33 and 26.4 %, respectively. Their structures were confirmed by ESI-TOF-MS, ^{1}H-NMR, and ^{13}C-NMR. The physicochemical analysis of peptide and lipopeptide showed that they were capable of condensing and protecting DNA from enzyme degradation at a ratio of 1:8 to DNA. The peptide and lipopeptide were found to be less efficient for transfection in HEK-293T cells because they required a high concentration (16,000 ng/µL). Nonetheless, peptide and lipopeptide concentrations of 250 - 16,000 ng/µL showed no toxicity to the cells.

Keywords: Gene delivery, NLS peptide, Lipopeptide, Solid phase peptide synthesis

Introduction

Gene therapy represents a transformative approach to treating genetic disorders, cancers, and other diseases by delivering therapeutic nucleic acids to target cells. The creation of novel delivery methods that guarantee safe, effective, and accurate targeting while overcoming biological obstacles, including enzymatic degradation, cellular absorption, and nuclear localization is necessary to accomplish this [1,2]. Non-viral vectors have attracted a lot of interest among different delivery methods because of their easier production, adaptable characteristics, and lower immunogenicity [3,4]. Among these, peptides have become highly effective means of delivering genes and addressing important biological problems.

Peptides, as short chains of amino acids, offer modular and multifunctional properties that make them particularly valuable in non-viral gene delivery systems. They can be designed to improve cellular absorption, stabilize nucleic acids, and ease endosomal escape. The capacity of cell-penetrating peptides (CPPs) to deliver therapeutic cargos into cells via receptor-mediated endocytosis or direct membrane penetration makes them

particularly noteworthy. Peptides are extremely versatile for a range of therapeutic applications since functional motifs can be added to them to accomplish tissue-specific or subcellular targeting [5,6]. These characteristics, along with their simplicity of synthesis and biocompatibility, make peptides a viable gene delivery vehicle.

One major barrier to effective gene delivery is enzymatic degradation during endocytosis. Peptides enriched with lysine (K) or arginine (R) residues form electrostatic complexes with negatively charged nucleic acids, shielding them from degradation and enhancing cellular uptake by increasing their affinity for negatively charged cell membranes [7,8]. After internalization, histidine (H)-rich motifs offer extra defense by buffering the endosomal environment and preventing enzymes like lysozyme and DNAse from breaking down the DNA-peptide complex [9]. Key intracellular delivery issues are addressed by these peptide-based approaches, and transfection efficiency has been demonstrated to increase significantly with additional optimization through structural changes [10,11].

Successful gene therapy frequently necessitates nuclear localization for the transcription of therapeutic nucleic acids in addition to cytoplasmic delivery. Short peptide sequences known as nuclear localization signals (NLS), such as the PKKKRKV motif from the simian virus 40 (SV40) large T antigen, are essential for directing genetic material into the nucleus. By interacting with shuttle proteins like importin α, these sequences facilitate active transport across the nuclear envelope and via nuclear pore complexes (NPCs) [12,13]. Gene carriers can accomplish accurate nucleus targeting by integrating NLS into peptide-based delivery methods, which greatly increases the transcriptional efficacy of given nucleic acids [14].

Building on the advantages of peptides, lipopeptides combine peptide functionality with lipid components to further enhance delivery efficiency. Lipopeptides are highly effective as non-viral vectors due to their lipid tail, which improves cellular absorption, endosomal escape, and gene release [15]. The characteristics of lipid tails, such as chain length, have a substantial impact on their performance. Tarwadi *et al.* [16] showed that the short lipopeptide C16-CKKHH may form persistent lipoplexes, which results in an 80-fold higher transfection efficiency in Cos7 cells than C12-CKKHH. Furthermore, by combining extracellular and intracellular delivery characteristics, the incorporation of NLS sequences into lipopeptide systems permits accurate nuclear targeting. This dual capability positions lipopeptides as highly versatile carriers for gene therapy, addressing key challenges such as enzymatic protection, endosomal escape, and nuclear localization.

The most common approach for synthesizing peptides and lipopeptides is solid-phase peptide synthesis (SPPS), a proven technique that allows for the very precise stepwise assembly of peptide sequences. Depending on the structure of the lipopeptide, the lipid tail can be incorporated either at the N-terminal or as a side chain modification to the peptide using a coupling agent [17,18]. Despite its effectiveness, SPPS has drawbacks, especially when dealing with long peptide sequences or hydrophobic modifications like those in lipopeptides. Peptide chain aggregation, inadequate coupling processes, and purification challenges are a few examples of potential problems [19,20]. Numerous approaches have been put out to deal with these problems. The use of small loading resins and coupling reagents, such as DIC/Oxyma that prevent racemization, can be useful in the synthesis of peptides or lipopeptides with long sequences [21].

Here, we synthesized, characterized, and evaluated the multifunctional novel peptide HKHK-PKKKRKV (P) and lipopeptide C16-HKHK-PKKKRKV (LP) (**Figure 1**) as a non-viral gene delivery vector. We added the HKHK sequence as a histidine-rich motif peptide to the short cationic peptide PKKKRKV, which is known as a monopartite NLS that can mediate nuclear uptake. Based on these studies, we suggest HKHK-PKKKRKV and C16-HKHK-PKKKRKV as prospective non-viral gene delivery vectors, which could help create safe and effective gene therapy strategies.

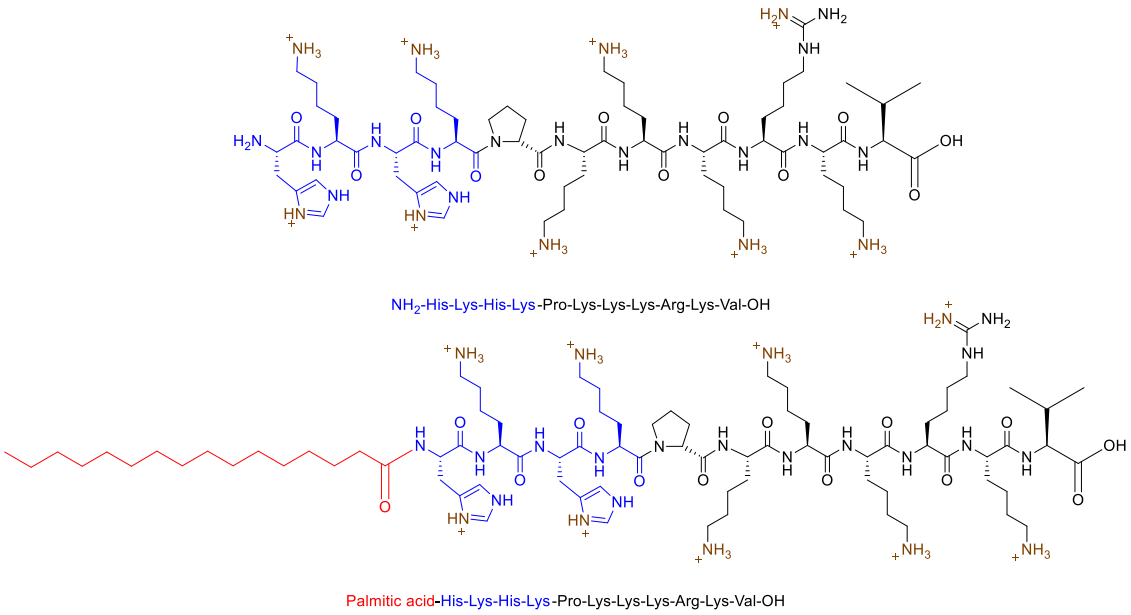

Figure 1 Chemical structure of peptide HKHK-PKKKRKV and lipopeptide C16-HKHK-PKKKRKV.

Materials and methods

Materials

The chemicals and reagents utilized in this research included 2-chlorotrityl chloride resin, *N,N'*-diisopropylcarbodiimide (DIC), 2-cyano-2-(hydroxyimino)acetate (Oxyma), dichloromethane (DCM), dimethylformamide (DMF), *N*-[(dimethylamino)-1*H*-1,2,3-triazolo-4,5-b]pyridine-1-yl-methylene]-*N*-methylmethanaaminium hexafluoro phosphate N-oxide (HATU), 1-hydroxy-7-azabenzotriazole (HOAt), *N,N*-diisopropyletilamine (DIPEA), Fmoc-L-Val-OH, Fmoc-L-Arg(Pbf)-OH, Fmoc-L-Pro-OH, Fmoc-L-Lys(Boc)-OH, Fmoc-L-His(Boc)-OH, trifluoroacetic acid (TFA), piperidine, palmitic acid, methanol, and *n*-hexane. All amino acids, coupling reagents, and resin were obtained from GL-Biochem in Shanghai, China.

The peptides were synthesized using the solid-phase peptide synthesis (SPPS) method with 2-chlorotrityl chloride resin as the solid support, employing the Fmoc strategy. The resin loading absorbance was measured using a TECAN Infinite Pro 200 UV-Vis spectrophotometer. Peptide purification was conducted via semi-preparative reverse-phase high-performance liquid chromatography (RP-HPLC), and the purity was analyzed with analytical RP-HPLC. Further analysis of the peptides and lipopeptides was carried out using a Waters Alliance e2695 system equipped with a photodiode array detector (PDA) and a LiChrospher 100 C-18 column (5 µM, 4.6×250 mm^2, COSMOSIL) at wavelengths of 210, 240, and 254 nm. Semi-preparative RP-HPLC utilized the same Waters Alliance e2695 system with a PDA detector and a larger C-18 column (5 µM, 10×250 mm, Jupiter). Structural characterization of lipopeptides was performed using Waters HR-TOF-ESI mass spectroscopy with Lockspray system, and NMR spectra were recorded on a Bruker Ascend spectrometer, involving ^{1}H at 700 MHz and ^{13}C at 175 MHz, using $CDCl_3$ as the solvent. The peptide was characterized using HR-TOF-ESI mass spectrometry and ^{1}H-NMR spectroscopy.

Peptide and lipopeptide synthesis

The linear peptide HKHK-PKKKRKV was synthesized manually using conventional Fmoc solid-phase peptide synthesis (SPPS) techniques. The synthesis utilized 2-chlorotrityl chloride resin (0.4 g, 0.6 mmol) as the solid support. Initially, the resin was swollen in dichloromethane (DCM, 10 mL) for 30 min in a rotary suspension mixer, followed by drying with an air pump. A solution containing Fmoc-Val-OH (1 eq., 0.6 mmol), DIPEA (2 eq., 1.2 mmol), and DCM (4 mL) was then added to the resin, and the mixture was shaken at room temperature for 30 min. The loading resin value was determined by incubating 0.6 mg of Fmoc-Val-OH-resin in 20 % piperidine/DMF (3 mL) for 30 min, and the absorbance was measured at 290 nm using UV-Vis spectroscopy. The resin was capped using a mixture of

methanol, DCM, and DIPEA (1.5:8:0.5, 10 mL) with shaking at room temperature for 2 cycles of 15 min each. Removal of the Fmoc protecting group from the first amino acid was achieved by treating the resin with 20 % piperidine in DMF (4 mL), followed by shaking the mixture for 2×5 min.

A solution of Fmoc-Lys(Boc)-OH (3 equiv.), HATU (3 eq.), HOAt (3 eq.), and DIPEA (6 eq.) in 5 mL DMF was added to the resin-AA_1-NH_2. The reaction mixture was shaken at room temperature for 4 h, then filtered and washed sequentially with DMF and DCM. Coupling efficiency was monitored using a chloranil test. This coupling and deprotection cycle were repeated to sequentially add 11 amino acids to the resin. Once the peptide chain was fully assembled, the linear peptides were cleaved from the resin using a mixture of 10 mL TFA:H_2O solution (95:5) with shaking at room temperature for 2×60 min. The resulting solution was collected, and the solvent was evaporated to yield the crude peptide NH_2-His-Lys-His-Lys-Pro-Lys-Lys-Arg-Lys-Val-OH as a pale white solid.

To attach the lipid moiety, the resin-linear peptide was reacted with a solution of palmitic acid (3 eq.), DIC (4 eq.), and Oxyma (4 eq.) in 4 mL DMF:DCM (1:1), with stirring at room temperature overnight. The lipopeptide was cleaved from the resin using 10 mL of a TFA:H_2O solution (95:5) with shaking at room temperature for 2×60 min. The filtrate was collected and evaporated to obtain yielding the crude C16-His-Lys-His-Lys-Pro-Lys-Lys-Arg-Lys-Val-OH., as a pale-yellow oil.

The crude peptide and lipopeptide were purified via semi-preparative RP-HPLC using an initial solvent system of H_2O/acetonitrile (95:5) with 0.1 % TFA, followed by a linear gradient to 80 % acetonitrile over 60 min at a flow rate of 2.0 mL/min with a C-18 column. Analytical RP-HPLC was employed to confirm purity using the same solvent system and gradient at a flow rate of 1.0 mL/min. The purified lipopeptide compound was characterized by ^{1}H-NMR, ^{13}C-NMR, and HR-TOF-ESI mass spectroscopy. The peptides were characterized by HR-TOF-ESI mass spectrometry and ^{1}H-NMR spectroscopy.

DNA isolation

The pCSII-EF-AcGFP plasmid was isolated using a QIAGEN® QIAprep Maxi Kit (Qiagen Pty. Ltd., Vic, Australia) in accordance with the supplier's instructions after being maintained in *E. coli* TOP10. After a single digestion with BamH1 (30 min, 90 V), the plasmid DNA was run on 1 % agarose gel electrophoresis, and its quantity and purity were assessed by spectrophotometric analysis at 260 and 280 nm. For storage, the purified plasmid DNA was frozen at −20 °C after being reconstituted in Milli-Q water (MQW).

DNA binding and complex stability assay

The binding affinity of the transfection agent/DNA was evaluated using the gel mobility shift assay, as previously described [16]. The DNA plasmid (1 μg/μL) was prepared in HGB (15 mM HEPES and 5.13 % w/v glucose) at pH 7.4 and combined with a transfection agent (1 μg/μL) in a series with a specific ratio (1:0.5, 1:1, 1:2, 1:3, 1:4 and 1:8). After incubating transfection agent/DNA complexes (20 μg/mL) for 30 min at room temperature, the sample (15 μL) was combined with 3 μL of loading buffer and subjected to 1 % agarose gel electrophoresis analysis. Following 30 min of agarose gel electrophoresis at 100 V, the DNA bands were visualized using UV transillumination. The stability of the transfection agent/DNA combination against DNase degradation was assessed by exposing the complex to DNaseI nucleases (Australia, Ambion, VIC and Turbo DNase). The transfection agent and plasmid DNA (1 μg/μL) are prepared in HGB pH 7.4 in the following series ratios: 1:0.5, 1:1, 1:2, 1:3, 1:4 and 1:8. After mixing and incubating the samples for 15 min at 37 °C with DNaseI (1 U/μg DNA), they were analyzed by 1 % agarose gel electrophoresis. UV transillumination at 320 nm was used to visualize DNA bands.

GFP expression

HEK-293T cells were cultivated on 96-well plates for 1×24 h until cell confluence reached 70 - 80 %. The number of cells put into the well was 10,000 - 50,000 cells for HEK-293T. The solution containing the pCSII-EF-AcGFP plasmid DNA complex and peptide/ lipopeptide with a certain ratio (1:0.5, 1:1, 1:2, 1:3, 1:4, 1:8, 1:16 and 1:32) that has been dissolved in HGB pH 7.4 as well as complete RPMI media was then inserted

into the well. Well plates were then incubated in an incubator at 37 °C with 5 % CO_2 supply and observed under a fluorescence microscope until a maximum of 3 days after the addition of DNA-peptide/lipopeptide complexes.

Cytotoxicity assay

HEK-293T cells were cultivated for 1×24 h until cell confluence reached 60 - 70 %, then peptide and lipopeptide were added in the amount of 200, 400, 800, 1,200 and 1,600 ng, as well as PEI-25,000 in the same amount as the control. HEK-293T cell line cultures in well plates that had been treated with the addition of peptide, lipopeptide, and cationic polymers were then grown for 24 h. The previous growth medium was discarded, and basal RPMI medium containing 0.5 mg/mL MTT solution was added afterward. Cells that have been added with MTT solution were incubated in an incubator at 37 °C for 4 h, and 20 % SDS solution was added to the well to stop the crystallization reaction. The well plate was incubated again under the same conditions for 24 h on a shaker, and then the culture results were observed by looking at the formation of formazan crystals through a microplate reader so that the absorbance value could be measured.

Results and discussion

Peptide and lipopeptide synthesis and structure characterization

Peptides (HKHK-PKKKRKV) and lipopeptides (C16-HKHK-PKKKRKV) were synthesized using the solid-phase peptide synthesis (SPPS) method with the Fmoc strategy (**Figure 2**). Peptide synthesis begins with the swelling of 2-chlorotryl chloride resin in dichloromethane for 30 min. To obtain a good loading value of the resin, the first amino acid, Fmoc-Val-OH, was bound to the resin using DIPEA base in dichloromethane solvent and shaken for 30 min using a rotatory suspension mixer. A good resin loading value ranges from 0.2 to 0.8 mmol/g [22]. In this study, a small resin loading value (0.1 to 0.2 mmol/g) was used to facilitate the long linear peptide synthesis process. Each peptide in the resin has a larger area and less aggregation efficacy when the loading resin value is minimal [21].

Resin capping is used to stop the following amino acid from entering the resin by sealing off the active side of the resin that does not bind to the first amino acid. The active side of the resin was capped using a DCM:methanol:DMF mixture. Deprotection of Fmoc-protecting groups was carried out using 20 % piperidine in DMF to form NH_2-L-Val-resin. Linear peptide elongation was achieved using 3 equivalents of HATU/HOAt coupling reagents and 6 equivalents of DIPEA base in DMF solution. A number of amino acid coupling reaction failures occurred during the synthesis process, particularly on the attachment of particular amino acids (such as arginine, lysine and histidine) and also at the attachment of residue into heptapeptidyl resin. This can be due to steric hindrance and possible aggregation, especially when synthesizing long peptides. These failures were identified by the resin that turns red when it was tested with chloranil after the completion of the coupling reaction. Double-to-triple coupling protocol and an overnight reaction time were used to get around this.

Following the binding of all amino acids to the resin to give peptide HKHK-PKKKRKV-resin. The linear peptides were released from the resin by cleavage accompanied by global deprotection of the amino acid side chain protecting groups with the employment of 95 % TFA in water, while lipopeptides are formed by reacting fatty acids with coupling reagents on the resin-peptide. The DIC/Oxyma coupling reagent (4 eq.) was used to further couple palmitic acid (C16) (3 eq.) to the N terminus of the peptide's linear chain on the resin. DIC/Oxyma reagent has a good ability in coupling reactions between fatty acids and peptides when compared to uranium/guanium-based coupling reagents because of its smaller structure that facilitates the reaction. Lipopeptides are released from the resin with the same reagent as peptides, which is 95 % TFA in water. Water is used as a scavenger. The peptide and lipopeptide crude were then concentrated with a rotary evaporator.

Peptide and lipopeptide crude were purified by semi-preparative RP-HPLC using an initial solvent system of H_2O/acetonitrile (95:5 %) with 0.1 % TFA, followed by a linear gradient to 80 % acetonitrile over 60 min at a flow rate of 2.0 mL/min with a C-18 column. Analytical RP-HPLC was employed to confirm purity using the same solvent system and gradient at a flow rate of 1.0 mL/min using a PDA detector. The yields of peptide and lipopeptide after purification were 33.4 and 26.4 %, respectively. The purity level and retention

times of the peptide and lipopeptide molecules were shown in **Table 1**.

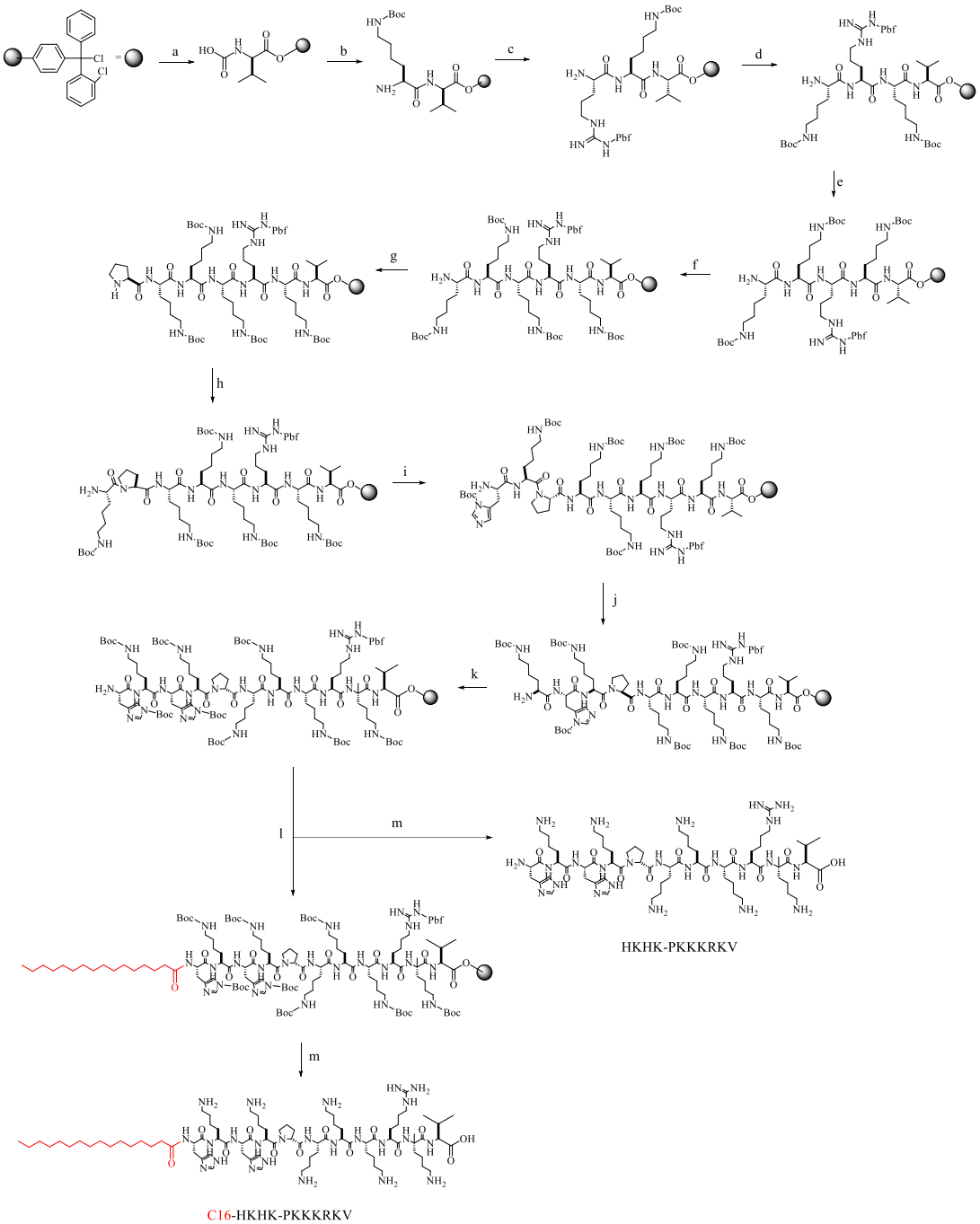

Figure 2 Solid phase peptide synthesis (SPPS) of lipopeptide C16-HKHK-PKKKRKV and peptide HKHK-PKKKRKV (a) (1) Fmoc-L-Val-OH (1 eq.), DIPEA (2 eq.), 4 mL DCM, 30 min, rt; (2) MeOH:DCM:DIPEA (15:80:5), 2×15 min; (3) 20 % piperidine in DMF, 2×5 min. (b, d, e, f, h and j). (1) Fmoc-L-Lys(Boc)-OH (3 eq.), HATU (3 eq.), HOAt (3 eq.), DIPEA (6 eq.), 5 mL DMF, 4 h, rt; (2) 20 % piperidine in DMF 2×5 min. (c). Fmoc-L-Arg(Pbf)-OH (3 eq.), HATU (3 eq.), HOAt (3 eq.), DIPEA (6 eq.), 5 mL DMF, 4 h, rt; (2) 20 % piperidine in DMF 2×5 min. (g). (1) Fmoc-L-Pro-OH (3 eq.), HATU (3 eq.), HOAt (3 eq.), DIPEA (6 eq.), 5 mL DMF, 4 h, rt; (2) 20 % piperidine in DMF 2×5 min. (i, k). (1) Fmoc-L-His(Boc)-OH (3 eq.), HATU (3 eq.), HOAt (3 eq.), DIPEA (6 eq.), 5 mL DMF, 4 h, rt; (2) 20 % piperidine in DMF 2×5 min. (l). (1) Palmitic acid (3 eq.); DIC (4 eq.), Oxyma (4 eq.), 5 mL DMF, overnight, rt; (2) 20 % piperidine in DMF 2×5 min. (m). Trifluoroacetic acid (TFA):H_2O (95:5) 2×60 min, rt.

Table 1 Retention time of analytical RP-HPLC spectra and purity of peptide and lipopeptide.

No	Compound	Retention Time (min)	Purity (%)
1	HKHK-PKKKRKV	20.577	96.8
2	C16-HKHK-PKKKRKV	16.303	98.8

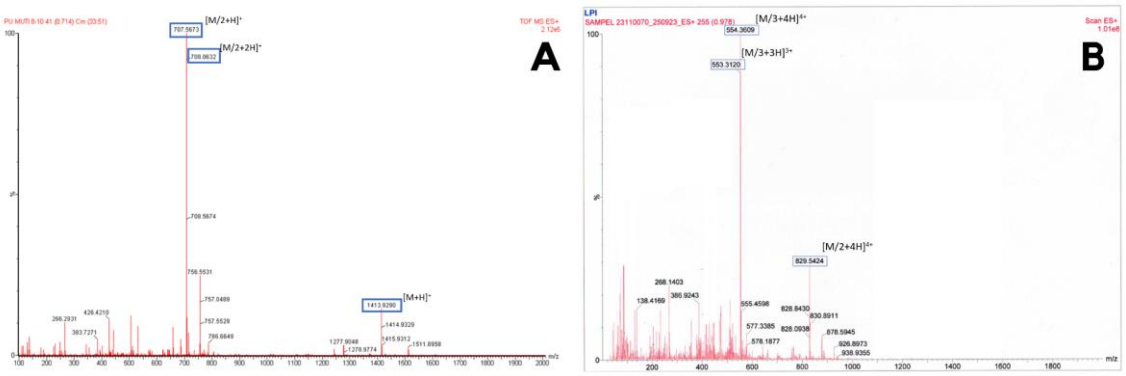

Figure 3 Mass spectrum of peptide HKHK-PKKKRKV (P) (A) and lipopeptide C16-HKHK-PKKKRKV (LP) (B).

The purified peptide and lipopeptide were confirmed by HR-TOF-ESI-MS at *m/z* 707.5673, which is $[M + 2H]^{2+}$ (calcd. *m/z* 707.4675) for peptide (**Figure 3(A)**) and *m/z* value of 554.3609, which is $[M/3 + 4H]^{4+}$ (calcd. *m/z* 554.3906) for lipopeptide (**Figure 3(B)**). Structural determination of the synthesized lipopeptide and peptide was carried out by ^{1}H-NMR (**Table 2**). From the ^{1}H-NMR spectrum of the peptide HKHK-PKKKRKV compound, 102 proton signals are produced. There are nine CHα signals confirmed by the chemical shift of 4.12 - 4.38 ppm. In addition, there are nine NH proton signals from amide bonds at a chemical shift of 7.88 - 7.92 ppm. Based on the ^{1}H-NMR spectrum data, the lipopeptide compound C16-HKHK-PKKKRKV produces 132 proton signals. The lipopeptide was confirmed by the presence of eleven CHα signals shown in the spectra. The NH_2 and OH peaks in the DMSO solvent frequently do not show up because these protons are readily swapped with the solvent's deuterium atoms (DMSO-d6), which results in their replacement by "ND" and "OD" groups, causing the peaks to disappear [23]. The ^{13}C-NMR spectrum of lipopeptide showed 12 typical signals for the carbon of the amide bond (**Table 3**). There are also 11 alpha carbon signals from each side chain of amino acid and fatty acid residues at a chemical shift of 14.4 - 140 ppm.

Table 2 ^{1}H-NMR spectra of compound HKHK-PKKKRKV and C16-HKHK-PKKKRKV in $(CD_3)_2SO$ and comparison with reference spectra.

Amino acids	HKHK-PKKKRKV	C16-HKHK-PKKKRKV	Biological magnetic resonance data bank [24]
	δ (ppm), multiplicity, J(Hz)	δ (ppm), multiplicity, J(Hz)	δH (ppm)
Palmitic acid			
2		2.07 - 2.09 (m)	
3		1.54 - 1.57 (m)	
4 - 6		1.34 - 1.35 (m)	
7 - 15		1.20 - 1.24 (m)	
16		0.85 - 0.87 (m)	

Amino acids	HKHK-PKKKRKV	C16-HKHK-PKKKRKV	Biological magnetic resonance data bank [24]
	δ (ppm), multiplicity, J(Hz)	δ (ppm), multiplicity, J(Hz)	δH (ppm)
Histidine			
α	4.12 - 4.16 (m)	4.18 - 4.21 (m)	4.17
β	3.06 - 3.10 (m)	3.02 - 3.05 (m)	3.13
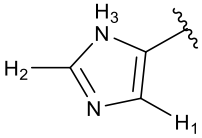	H_1 = 7.25 - 7.27 (m) H_2 = 8.95 - 8.96 (d) J = 7 H_3 = 8.58 - 8.62 (d) J = 7	H_1 = 7.45 - 7.47 (m) H_2 = 8.46 - 8.47 (d) J = 7 H_3 = 8.64 - 8.70 (d) J = 7	H_1 = 7.08 H_2 = 7.82 H_3 = 8.86
Lysine			
α	4.24 - 4.28 (m)	4.20 - 4.27 (m)	4.25
β	1.62 - 1.68 (m)	1.63 - 1.66 (m)	1.77
2	1.28 - 1.33 (m)	1.24 - 1.29 (m)	1.36
3	1.50 - 1.54 (m)	1.54 - 1.57 (m)	1.60
4	2.72 - 2.78 (m)	2.75 - 2.78 (m)	2.91
Histidine			
α	4.12 - 4.16 (m)	4.18 - 4.21 (m)	4.17
β	3.06 - 3.10 (m)	3.14 - 3.15 (m)	3.13
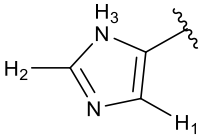	H_1 = 7.25 - 7.27 (m) H_2 = 8.95 - 8.96 (d) J = 7 H_3 = 8.58 - 8.62 (d) J = 7	H_1 = 7.45 - 7.47 (m) H_2 = 8.46 - 8.47 (d) J = 7 H_3 = 8.64 - 8.70 (d) J = 7	H_1 = 7.08 H_2 = 7.82 H_3 = 8.86
Lysine			
α	4.24 - 4.28 (m)	4.20 - 4.27 (m)	4.25
β	1.62 - 1.68 (m)	1.63 - 1.66 (m)	1.77
2	1.28 - 1.33 (m)	1.24 - 1.29 (m)	1.36
3	1.50 - 1.54 (m)	1.54 - 1.57 (m)	1.60
4	2.72 - 2.78 (m)	2.75 - 2.78 (m)	2.91
Proline			
α	4.37 - 4.38 (m)	4.34 - 4.35 (m)	4.38
β	2.04 - 2.08 (m)	2.04 - 2.06 (m)	2.07
γ	2.00 - 2.04 (m)	2.02 - 2.03 (m)	2.00
δ	3.80 - 3.82 (m)	3.51 - 3.55 (m)	3.63
Lysine			
α	4.24 - 4.28 (m)	4.20 - 4.27 (m)	4.25

Amino acids	HKHK-PKKKRKV	C16-HKHK-PKKKRKV	Biological magnetic resonance data bank [24]
	δ (ppm), multiplicity, J(Hz)	δ (ppm), multiplicity, J(Hz)	δH (ppm)
β	1.62 - 1.68 (m)	1.63 - 1.66 (m)	1.77
2	1.28 - 1.33 (m)	1.24 - 1.29 (m)	1.36
3	1.50 - 1.54 (m)	1.54 - 1.57 (m)	1.60
4	2.72 - 2.78 (m)	2.75 - 2.78 (m)	2.91
Lysine			
α	4.24 - 4.28 (m)	4.20 - 4.27 (m)	4.25
β	1.62 - 1.68 (m)	1.63 - 1.66 (m)	1.77
2	1.28 - 1.33 (m)	1.24 - 1.29 (m)	1.36
3	1.50 - 1.54 (m)	1.54 - 1.57 (m)	1.60
4	2.75 - 2.78 (m)	2.75 - 2.78 (m)	2.91
Lysine			
α	4.30 - 4.31 (m)	4.20 - 4.27 (m)	4.25
β	1.62 - 1.68 (m)	1.63 - 1.66 (m)	1.77
2	1.28 - 1.33 (m)	1.24 - 1.29 (m)	1.36
3	1.50 - 1.54 (m)	1.54 - 1.57 (m)	1.60
4	2.72 - 2.78 (m)	2.75 - 2.78 (m)	2.91
Arginine			
α	4.37 - 4.38 (m)	4.41 - 4.46 (m)	4.28
β	1.72 - 1.74 (m)	1.63 - 1.66 (m)	1.79
γ	1.50 - 1.54 (m)	1.52 - 1.54 (m)	1.54
δ	3.16 - 3.18 (m)	3.28 - 3.30 (m)	3.10
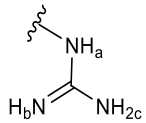	Ha = - Hb = 7.78 - 7.80 (m) Hc = 6.95 - 6.96 (m)	Ha = - Hb = 7.70 - 7.72 (m) Hc = 6.95 - 6.96 (m)	
Lysine			
α	4.30 - 4.31 (m)	4.20 - 4.27 (m)	4.25
β	1.62 - 1.68 (m)	1.63 - 1.66 (m)	1.77
2	1.28 - 1.33 (m)	1.24 - 1.29 (m)	1.36
3	1.50 - 1.54 (m)	1.54 - 1.57 (m)	1.60
4	2.72 - 2.78 (m)	2.75 - 2.78 (m)	2.91

Amino acids	HKHK-PKKKRKV	C16-HKHK-PKKKRKV	Biological magnetic resonance data bank [24]
	δ (ppm), multiplicity, J(Hz)	δ (ppm), multiplicity, J(Hz)	δH (ppm)
Valine			
α	4.18 - 4.20 (m)	4.14 - 4.16 (m)	4.16
β	1.90 - 1.92 (m)	2.00 - 2.01 (m)	1.98
γ	0.86 - 0.88 (m)	0.85 - 0.87 (m)	0.81
δ	0.86 - 0.88 (m)	0.85 - 0.87 (m)	0.80

Table 3 ^{13}C-NMR spectra of compound C16-HKHK-PKKKRKV in $(CD_3)_2SO$ and comparison with reference spectra.

Amino acid	C16-HKHK-PKKKRKV	Biological magnetic resonance data bank [24]
	^{13}C (ppm)	^{13}C (ppm)
Palmitic acid		
CO	174.4	
2	35.6	
3	25.6	
4	26.8	
5	26.9	
6 - 12	29.5	
13	29.3	
14	31.1	
15	22.6	
16	14.4	
Histidine		
CO	174.4	176.6
α	53.3	57.4
β	30.4	30.6
2	140.0	138.8
3	135.0	134.4
4	120.8	119.5
Lysine		
CO	172.0	176.6
α	57.7	56.9
β	31.7	32.7
2	22.4	24.9

Amino acid	C16-HKHK-PKKKRKV	Biological magnetic resonance data bank [24]
	^{13}C (ppm)	^{13}C (ppm)
3	29.0	28.9
4	39.7	41.9
Histidine		
CO	174.4	176.6
α	53.2	57.4
β	30.5	30.6
2	140.0	138.8
3	134.9	134.4
4	120.2	119.5
Lysine		
CO	172.2	176.6
α	57.8	56.9
β	31.7	32.7
2	22.1	24.9
3	29.0	28.9
4	39.8	41.9
Proline		
CO	173.6	176.6
α	66.2	63.3
β	29.6	31.8
γ	24.7	27.2
δ	51.0	50.3
Lysine		
CO	172.8	176.6
α	57.9	56.9
β	31.7	32.7
2	22.5	24.9
3	29.1	28.9
4	39.9	41.9
Lysine		
CO	173.0	176.6
α	58.0	56.9
β	31.7	32.7

Amino acid	C16-HKHK-PKKKRKV	Biological magnetic resonance data bank [24]
	^{13}C (ppm)	^{13}C (ppm)
2	22.6	24.9
3	29.2	28.9
4	40.1	41.9
Lysine		
CO	173.2	176.6
α	58.1	56.9
β	31.7	32.7
2	22.6	24.9
3	29.3	28.9
4	40.2	41.9
Arginine		
CO	173.6	176.6
α	29.0	56.7
β	23.9	30.6
γ	39.1	27.2
δ	158.3	43.1
Lysine		
CO	173.0	176.6
α	58.1	56.9
β	31.7	32.7
2	22.4	24.9
3	29.4	28.9
4	40.3	41.9
Valine		
CO	174.0	175.6
α	63.5	62.5
β	30.1	32.6
γ	18.5	21.5
δ	19.0	21.3

Peptide/lipopeptide-DNA binding studies

The ability of lipopeptides and peptides to condense or interact with DNA was performed using a gel retardation assay. Peptide HKHK-PKKKRKV and lipopeptide C16-HKHK-PKKKRKV showed that the DNA-lipopeptide complex with a ratio of 1:8 successfully complexed DNA well (**Figure 5(A)**), which was characterized by the absence of visible DNA

bands. Peptides are more effective in complexing DNA at lower ratios than lipopeptides. The hazy DNA band seen in the lipopeptide sample with a ratio of 1:4 to DNA indicates the peptide is more effective in complexing DNA at a lower ratio than the lipopeptide. This can occur because peptides are more cationic, so they bind more strongly to DNA, which has anionic properties. The lipid part of the lipopeptide can cause steric hindrance, i.e., its large hydrophobic tail can prevent the molecule from getting closer to the DNA and forming a tight complex. This greater distance can weaken the electrostatic interactions required for DNA condensation. Meanwhile, peptides without lipid tails can more closely engage with DNA.

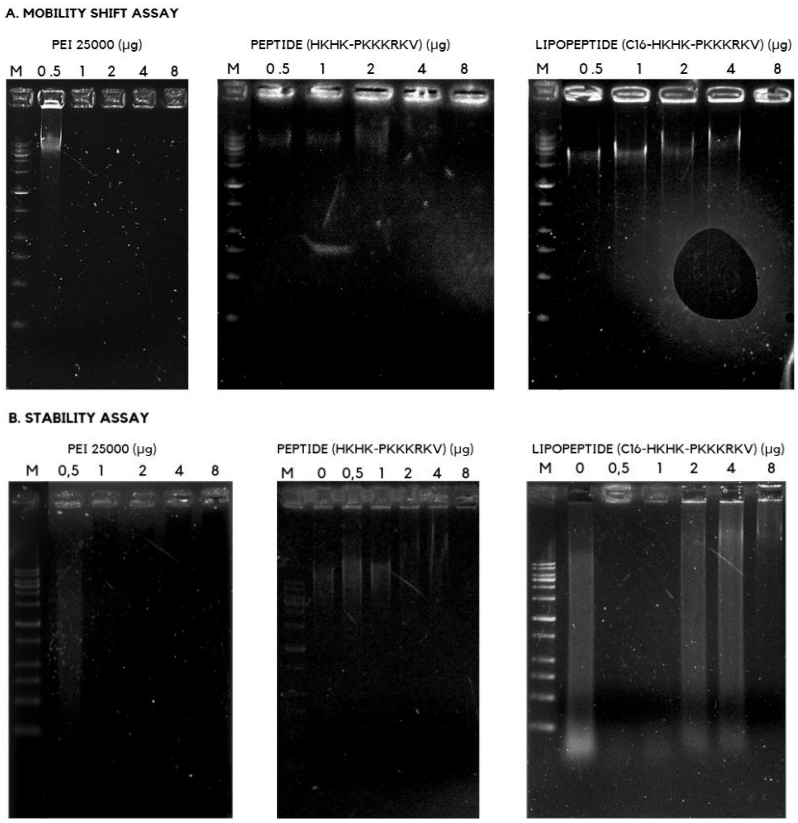

Figure 5 DNA-transfection agent binding studies (A). DNA mobility shift assay (B). DNA-transfection agent stability against DNase degradation (M: DNA marker 1 kb plus, DNA: Plasmid pCSII-EF-AcGFP 500 ng/µL).

The ability to effectively bind and condense DNA into a stable complex is essential to protect DNA from enzymatic degradation during the delivery process to the cell nucleus. The stability of DNA-peptide/lipopeptide complexes against enzymes is seen by stability tests against DNase. The addition of the DNase enzyme acts to degrade free DNA through the degradation of DNA phosphodiester bonds. Stability testing on peptide HKHK-PKKKRKV and lipopeptide C16-HKHK-PKKKRKV showed that at ratios below 1:8, only part of the DNA was successfully condensed by the peptide/lipopeptide (**Figure 5(B)**), while the rest was free to migrate and degraded by DNAse, then mixed with RNA to form smear bands. However, the peptide did not show any visible free RNA at the bottom of the gel at all ratios. Peptides protect DNA better than lipopeptides because not all DNA is degraded into RNA.

In contrast to peptide and lipopeptide, PEI 25000 effectively compacted DNA at a ratio of 1:0.5, as evidenced by the absence of free DNA bands in agarose gel electrophoresis (**Figure 5A**). Since a cationic polymer, PEI 25000 can efficiently complex DNA even at low concentrations. As shown in **Figure 5(B)**, there was no formation of smear bands at ratios higher than 1:05 to DNA. This suggests that because the cationic polymer could encapsulate and shield DNA from enzyme degradation, the DNA-PEI 25000 complex can successfully prevent DNA from enzyme degradation.

GFP expression

The DNA used as the genetic material delivered in this test is plasmid pCSII-EF-AcGFP. This plasmid has a gene encoding Green Fluorescent Protein (GFP), which can provide fluorescent light intensity to facilitate the process of observing the success of cell transfection. The results of the transfection of plasmid pCSII-EF-AcGFP mediated by peptide, lipopeptide, and PEI 25000 as a positive control into the HEK-293T cell line can be seen in **Figure 6**. PEI-25,000 cationic polymer with the ratio to DNA (1:0.5, 1:1, 1:2, 1:3 and 1:4) or at a concentration of 2.5 - 20 ppm successfully expresses the GFP-encoding gene very well on almost the entire surface of HEK-293T cells. However, at high concentrations or at a ratio of 1:16 and 1:32, it did not show any green luminescence on the entire cell surface. This is because, at these concentrations, the cells were lysed/dead due to the toxic nature of PEI to the cells.

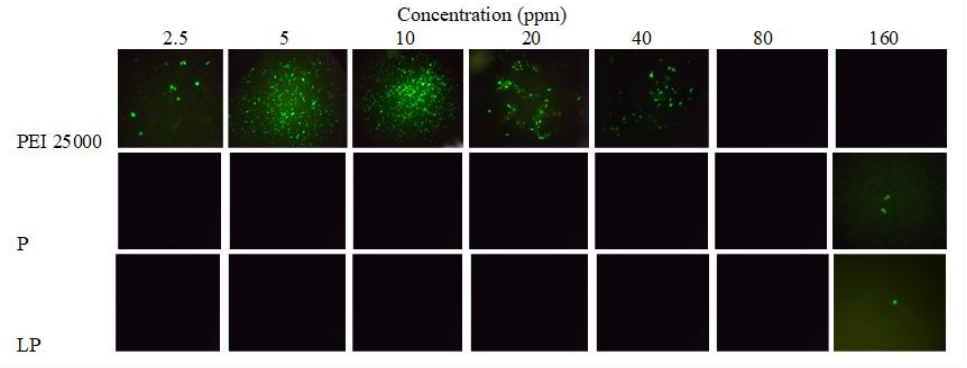

Figure 6 Transfection results of pCSII-EF-AcGFP plasmid (500 ng/µL) into HEK293T cell line with peptide (P); lipopeptide (LP), and positive control (PEI 25000).

Peptide (HKHK-PKKKRKV) and lipopeptide (C16-HKHK-PKKKRKV) successfully transfected cells at a ratio of 1:32 to DNA or at a peptide/lipopeptide concentration of 160 ppm with a relatively small amount. When compared to the positive control (PEI 25000), which can transfect cells at a low concentration ratio (1:0.5 - 1:8). Peptide and lipopeptide are not as effective as PEI 25000 in delivering DNA. This could be because peptides have a lower cationic charge compared to PEI, so that the condensation of lipopeptides/peptides with DNA becomes less optimal and cell transfection is only successful at high enough concentrations. Previously, it has been reported that cationic gemini lipopeptides that have been incorporated into conventional liposomes, containing DOPE and DOTAP, substantially improve transfection efficiency, superior to the traditional liposomes, DOTAP-DOPE [25]. Therefore, peptide/lipopeptide formulation with the addition of lipids to form stable liposomes may be necessary to enhance its activity.

Cytotoxicity analysis

The results of the cytotoxicity test of PEI-25000 as a control, as well as peptide and lipopeptide, can be seen in the graph presented in **Figure 7**. Peptides and lipopeptides resulted in cell viability close to 100 %. Peptides showed cell viability reaching ~ 86 % at high concentrations (16,000 ng/µL), while lipopeptides were more toxic than peptides, with cell viability decreasing to ~ 75 % at the same concentration. These results are in accordance with Wang *et al.* [18], which utilized C18 in the NLS-R8 peptide as a cell-penetrating peptide. In their study, lipopeptides with stearic fatty acids had lower cell viability when compared to peptides without fatty acids. Lipids in lipopeptides can facilitate the insertion of lipopeptides into cell membranes by increasing the permeability of cell membranes to ions and molecules and disrupting cellular homeostasis.

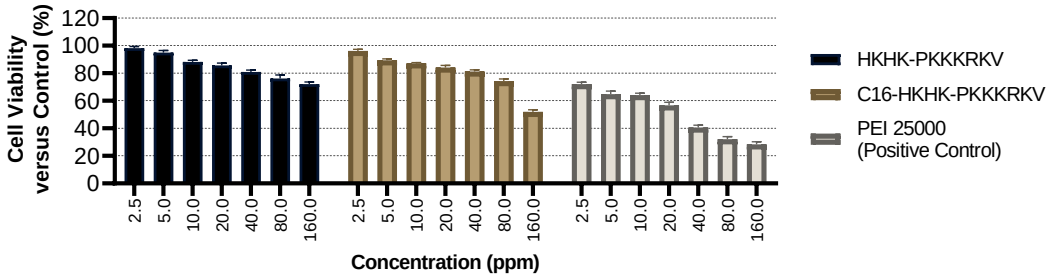

Figure 7 Cytotoxity of peptide (viability ~ 86 %), lipopeptide (viability ~ 75 %), and PEI-25000 (viability ~ 50 %) using MTT assay method.

The cytotoxicity test of the cationic polymer PEI-25000 as a positive control with MTT resulted in an average cell viability value of 50 %. Despite producing high gene expression, PEI-25000 is highly toxic. The toxicity of large molecular weight cationic polymers such as PEI-25,000 is caused by only part of the PEI molecule being able to form a complex with DNA and the other remaining in the cell. Free PEI molecules in the cell will cause necrosis and apoptosis in the cell [26].

Conclusions

Peptide HKHK-PKKKRKV and lipopeptide compound C16-HKHK-PKKKRKV were successfully synthesized using the solid-phase peptide synthesis method. The use of HATU/HOAt reagents as coupling reagents between amino acids and DIC/Oxyma as coupling reagents between peptides and fatty acids is known to facilitate the synthesis process. In addition, the use of small resin loading values is also necessary to facilitate the synthesis of peptides and lipopeptides with long amino acid residues. Peptides and lipopeptides were obtained with high purity (> 95 %) and confirmed through characterization using HR-TOF-ESI-MS and ^{1}H-NMR and ^{13}C-NMR. The physicochemical properties of peptide and lipopeptide showed that they were capable of condensing DNA and protecting DNA from enzyme degradation at a ratio of 1:8 to DNA. Peptide and lipopeptide in concentrations of 2.5 - 20 ppm were found to be less effective as transfection agents in HEK-293T cell lines because a large amount of peptide/lipopeptides was required (160 ppm, or equivalent to 1:32 to DNA). Meanwhile, peptide and lipopeptide in concentrations of 2.5 - 160 ppm were not toxic to HEK-293T cell lines.

Acknowledgements

Author would like to express gratitude to research grants of this research was funded by LPDP through RIIM-BRIN 2023 (Grant Number: 124/IV/KS/11/2023 dan 5994/UN6.3.1/PT.00/2023) and KEMENRISTEK DIKTI Indonesia, through Penelitian Tesis Magister (PTM) scheme (Grant number: 3973/UN6.3.1/PT.00/2024) and for financial support.

References

[1] SL Ginn, M Mandwie, IE Alexander, M Edelstein and MR Abedi. Gene therapy clinical trials worldwide to 2023 - an update. *The Journal of Gene Medicine* 2024; **26(8)**, 3721.

[2] JA Kulkarni, D Witzigmann, SB Thomson, S Chen, BR Leavitt, PR Cullis and R van der Meel. The current landscape of nucleic acid therapeutics. *Nature Nanotechnology* 2021; **16(6)**, 630-643.

[3] C Wang, C Pan, H Yong, F Wang, T Bo, Y Zhao, B Ma, W He and M Li. Emerging non-viral vectors for gene delivery. *Journal of Nanobiotechnology* 2023; **21(1)**, 272.

[4] L Jiao, Z Sun, Z Sun, J Liu, G Deng and X Wang. Nanotechnology-based non-viral vectors for gene delivery in cardiovascular diseases. *Frontiers in Bioengineering and Biotechnology* 2024; **12**, 1349077.

[5] S Tarvirdipour, M Skowicki, CA Schoenenberger and CG Palivan. Peptide-assisted nucleic acid delivery systems on the rise. *International Journal of Molecular Sciences* 2021; **22(16)**, 9092.

[6] Y Liu, Z Zhao and M Li. Overcoming the cellular barriers and beyond: Recent progress on cell penetrating peptide modified nanomedicine in combating physiological and pathological

barriers. *Asian Journal of Pharmaceutical Sciences* 2022; **17(4)**, 523-543.

[7] R Hadianamrei and X Zhao. Current state of the art in peptide-based gene delivery. *Journal of Controlled Release* 2022; **343**, 600-619.

[8] J Yang and GF Luo. Peptide-based vectors for gene delivery. *Chemistry* 2023; **5(3)**, 1696-1718.

[9] P Belguise-Valladier and JP Behr. Nonviral gene delivery: Towards artificial viruses. *Cytotechnology* 2001; **35(3)**, 197-201.

[10] J He, S Xu, Q Leng and AJ Mixson. Location of a single histidine within peptide carriers increases mRNA delivery. *The Journal of Gene Medicine* 2021; **23(2)**, 3295.

[11] A Kichler, AJ Mason and B Bechinger. Cationic amphipathic histidine-rich peptides for gene delivery. *Biochim Biophys Acta* 2006; **1758(3)**, 301-307.

[12] J Lu, T Wu, B Zhang, S Liu, W Song, J Qiao and H Ruan. Types of nuclear localization signals and mechanisms of protein import into the nucleus. *Cell Communication and Signaling* 2021; **19(1)**, 60.

[13] H Bai, GMS Lester, LC Petishnok and DA Dean. Cytoplasmic transport and nuclear import of plasmid DNA. *Bioscience Reports* 2017; **37(6)**, BSR20160616.

[14] EM Cross, N Akbari, H Ghassabian, M Hoad, S Pavan, D Ariawan, CM Donnelly, E Lavezzo, GF Petersen, JK Forwood and G Alvisi. A functional and structural comparative analysis of large tumor antigens reveals evolution of different importin α-dependent nuclear localization signals. *Protein Science* 2024; **33(2)**, e4876.

[15] IW Hamley. Lipopeptides: From self-assembly to bioactivity. *Chemical Communications* 2015; **51(41)**, 8574-8583.

[16] Tarwadi, JA Jazayeri, RJ Prankerd and CW Pouton. Preparation and *in vitro* evaluation of novel lipopeptide transfection agents for efficient gene delivery. *Bioconjugate Chemistry* 2008; **19(4)**, 940-950.

[17] W Zeng, KJ Horrocks, G Robevska, CY Wong, K Azzopardi, M Tauschek, RM Robins-Browne and DC Jackson. A modular approach to assembly of totally synthetic self-adjuvanting lipopeptide-based vaccines allows conformational epitope building. *The Journal of Biological Chemistry* 2011; **286(15)**, 12944-12951.

[18] HY Wang, JX Chen, YX Sun, JZ Deng, C Li, XZ Zhang and RX Zhuo. Construction of cell-penetrating peptide vectors with N-terminal stearylated nuclear localization signal for targeted delivery of DNA into the cell nuclei. *Journal of Controlled Release* 2011; **155(1)**, 26-33.

[19] M Paradís-Bas, J Tulla-Puche and F Albericio. The road to the synthesis of "difficult peptides." *Chemical Society Reviews* 2016; **45(3)**, 631-654.

[20] LK Mueller, AC Baumruck, H Zhdanova and AA Tietze. Challenges and perspectives in chemical synthesis of highly hydrophobic peptides. *Frontiers in Bioengineering and Biotechnology* 2020; **8**, 162.

[21] AT Hidayat, R Maharani, AY Chaerunisaa, FF Masduki, R Aditama, H Setiawana and Tarwadi. Synthesis, characterization, and *in vitro* evaluation of short cationic peptides for gene delivery vehicle candidate. *Current Bioactive Compounds* 2024; **20(3)**, 14-24.

[22] CW Chan and PD White. *Fmoc solid phase peptide synthesis.* Oxford University Press, Nottingham, 2000.

[23] L Cseri, S Kumar, P Palchuber and G Szekely. NMR chemical shifts of emerging green solvents, acids, and bases for facile trace impurity analysis. *ACS Sustainable Chemistry & Engineering* 2023; **11(14)**, 5696-5725.

[24] JC Hoch, K Baskaran, H Burr, J Chin, HR Eghbalnia, T Fujiwara, MR Gryk, T Iwata, C Kojima, G Kurisu, D Maziuk, Y Miyanoiri, JR Wedell, C Wilburn, H Yao and M Yokochi. Biological magnetic resonance data bank. *Nucleic Acids Research* 2023; **51(D1)**, D368-D376.

[25] V Ravula, YL Lo, LF Wang and SV Patri. Gemini lipopeptide bearing an ultrashort peptide for enhanced transfection efficiency and cancer-cell-specific cytotoxicity. *ACS Omega* 2021; **6(35)**, 22955-22968.

[26] H Zhang, Z Chen, M Du, Y Li and Y Chen. Enhanced gene transfection efficiency by low-dose 25 kDa polyethylenimine by the assistance of 1.8 kDa polyethylenimine. *Drug Delivery* 2018; **25(1),** 1740-1745.